Accepted Manuscript

An innovative technique for estimating water saturation from capillary pressure in clastic reservoirs

Lukumon Adeoti, Elijah Adebowale Ayolabi, Logan James

PII: S1464-343X(17)30321-7

DOI: 10.1016/j.jafrearsci.2017.08.004

Reference: AES 2986

To appear in: *Journal of African Earth Sciences*

Received Date: 5 August 2016

Revised Date: 2 July 2017

Accepted Date: 9 August 2017

Please cite this article as: Adeoti, L., Ayolabi, E.A., James, L., An innovative technique for estimating water saturation from capillary pressure in clastic reservoirs, *Journal of African Earth Sciences* (2017), doi: 10.1016/j.jafrearsci.2017.08.004.

An innovative technique for estimating water saturation from capillary pressure in clastic reservoirs

Lukumon Adeoti [1]*, Elijah Adebowale Ayolabi [1], Logan James[2]
[1]Department of Geosciences, University of Lagos, Lagos, Nigeria
[2] Chevron Nigeria Limited
* Corresponding author. Tel.: +2348034739175.
E-mail address: lukuade@yahoo.com (L. Adeoti).

ABSTRACT

A major drawback of old resistivity tools is the poor vertical resolution and estimation of hydrocarbon when applying water saturation (S_w) from historical resistivity method. In this study, we have provided an alternative method called saturation height function to estimate hydrocarbon in some clastic reservoirs in the Niger Delta. The saturation height function was derived from pseudo capillary pressure curves generated using modern wells with complete log data. Our method was based on the determination of rock type from log derived porosity-permeability relationship, supported by volume of shale for its classification into different zones. Leverette-J functions were derived for each rock type. Our results show good correlation between S_w from resistivity based method and S_w from pseudo capillary pressure curves in wells with modern log data. The resistivity based model overestimates S_w in some wells while S_w from the pseudo capillary pressure curves validates and predicts more accurate S_w. In addition, the result of S_w from pseudo capillary pressure curves replaces that of resistivity based model in a well where the resistivity equipment failed. The plot of hydrocarbon pore volume (HCPV) from J-function against HCPV from Archie shows that wells with high HCPV have high sand qualities and vice versa. This was further used to predict the geometry of stratigraphic units. The model presented here freshly addresses the gap in the estimation of S_w and is applicable to reservoirs of similar rock type in other frontier basins worldwide.

Keywords: Water saturation, Leverette-J functions, Reservoir, Core data, Pseudo capillary pressure curves

1. Introduction

A common shortcoming with conventional resistivity methods is poor resolution in thinly bedded formations (laminations occur within less than 1m interval). Other problems include the effects of the mud filtrate invasion, water imbibition processes, clay excess conductivity and determination of the Archie saturation exponent "n" that is itself wettability dependent during imbibition (Harrison and Jing, 2001). These shortcomings are challenging and always lead to inaccurate calculation of S_w. Water saturation (S_w) is conventionally from electrical resistivity methods or from capillary pressure, which can equally be called saturation height functions. Archie saturation equation, which relates resistivity to porosity, water saturation and various rock parameters, is the industry standard for clean formations and the foundation of quantitative petrophysics (Archie, 1942). All other expressions for estimating water saturation from resistivity log responses for example, laminated shale model, dispersed shale model, structural shale model simandoux model (Simandoux,1963), indonesia model (Poupon and Leveaux, 1971) etc. developed for shaly sand analysis are based on the Archie relationship. As the amount of shale decreases to zero, the shaly sand equations all revert to this same algorithm (Goetz, 2002).

The shaly sand analyses are based on the distribution of shale or clay in the sand. Most logging tools average formation response over 2 ft. to 4 ft. vertical intervals (Dewan, 1983). In these 'unresolvable' intervals, shale or clay may be disposed in the sand in three ways or in combinations thereof; laminated, dispersed, and structural (Dewan 1983). This distribution has led to the development of commonly used shaly sand models such as laminated shale, dispersed shale, structural shale and simandoux (Dewan,1983), while shaly sand models based on cation exchange capacity (CEC) are Waxman-smiths and dual water (Bateman, 1990). The measured resistivity of the reservoir can be affected by other factors, such as low-salinity pore fluids or conductive minerals like chlorite (Joanne et al., 2014) and more commonly, by the presence of shale and clay minerals(Archie, 1942). When clay minerals are present in a sandstone reservoir especially when they coat the quartz grains, the measured total resistivity can be lowered as clays exhibit an excess conductivity (Joanne et al., 2014). This excess conductivity associated with the clays can counteract the increase in resistivity caused by the presence of hydrocarbons in the pore space, resulting in the resistivity across the hydrocarbon-bearing zones becoming indistinguishable from the lower-resistivity water-bearing zones. This phenomenon is commonly referred to as 'low-resistivity pay' or 'low-resistivity contrast (Worthington, 2000). Hence, there is need for an alternative method of evaluating the S_w in lieu of the conventional resistivity method.

The saturation height functions can be from special core data and/ or logs. The relationship between capillary pressure and water saturation offers a technique to estimate water saturation versus depth which is independent of wire line logs, and provides the ability to calibrate log-derived saturations. Saturation height models, if implemented successfully, would also eliminate or minimize the uncertainties associated with electrical parameters measurements (Amabeoku et al., 2005). When the conventional methods for the calculation of the water saturation (S_w) profile in the reservoir are not reliable for different reasons, a viable alternative is the calculation based on capillary pressure (P_c) curve. If the capillary pressure in a point were known, water saturation could be calculated without the need of any standard resistivity model

whenever free water level (FWL), fluid density of hydrocarbon were determined with certain precision (Juan et al., 2003).

To test the validity of the saturation height functions over conventional methods, a case study area where several wells have drilled is chosen. The study area lies within the Niger Delta where vast commercial accumulation of oil and gas is produced from sandstones, limestones or dolomites (Schlumberger, 1989). In main reservoir rocks of the Niger Delta are within the Agbada Formation, which includes alternating sandstones and shales varying in thickness from 100 ft. (30 m) to 15,000 ft. (4600 m) (Short and Stauble, 1967). The poor vertical resolution of old resistivity tools in some of the wells in the Orire Field, Niger Delta could not adequately account for the hydrocarbon in the G-01 sand. Hence, the alternative capillary based method of generating water saturation is proposed. In this study, we have used developed rock type from log-derived permeability – porosity relationship supported by volume of shale to classify the lithology and rock type zones. To achieve this, the Leverett J – function was applied for the analysis. The method here provides an innovative technique for properly estimating hydrocarbon in the subsurface.

2. Geology of the study area.

The Niger Delta (Fig.1a) is a prograding depositional complex within the Cenozoic Formation of Southern Nigeria. The Niger Delta covers an area of about 75,000 square kilometers and it extends from the Calabar Flank and the Abakaliki Trough in Eastern Nigeria to the Benin Flank in the west and opens to the Atlantic Ocean in the southern territory (Fig. 1a). The delta extends into Gulf of Guinea from the Benue Trough and Anambra Basin Provinces (Evamy et al., 1978). From the Eocene to the present, the delta has prograded southwestwardly resulting in depobelts that represent the most active portion of the delta at each developmental stage (Doust and Omatsola, 1990).

There are three major lithostratigraphic units in the Niger Delta: Akata, Agbada and Benin Formation (Short and Stauble, 1967; Fig.2). The Akata Formation is a shale unit recognised as the major source of oil and gas (Evamy et al., 1978; Ekweozor et al., 1979; Ekweozor and Okoye, 1980; Lambert-Aikhionbare and Ibe, 1984; Doust and Omatsola, 1990). The Agbada Formation consists of sands and shales units, while the Benin Formation is composed mainly of sands (Weber and Daukoru, 1975; Frost, 1977; Evamy et al., 1978; Ejedawem *et al.,* 1979; Ekweozor and Okoye, 1980; Ekweozor and Daukoru, 1984; Lambert-Aikhionbare and Ibe, 1984; Doust and Omatsola, 1990; Stacher, 1995; Haack et al, 1997). These lithostratigraphic units form one of the largest regressive deltas in the world with an area of some 500,000 km^2 (Kulke, 1995), a sediment volume of about 500,000 km^3 and a sediment thickness of more than 10 km in the basin depocentre (Kaplan *et al.,* 1994).

The study area (Fig. 2) falls within the offshore part of the Niger Delta (Agbada Formation). G-01 sand used for analysis in Field X is characterized by shoreface sands, which are deposited in high energy environment (Peter and Darwin, 1982). Shoreface sands are divided into three: upper shoreface sand, lower shoreface sand, and middle shoreface sand (Avbobvo, 1978; Doust and Omatola, 1990; Kulke, 1995). The G-01 sand predominantly falls between lower shoreface and middle shoreface but G-01 sand in well 41 experiences upper shoreface with channel cut. Upper shoreface sand has been characterized by trough-cross bedded fine to medium grained sandstones with very little

bioturbation (Adeyemo et al., 2005). The cross bedded upper-shore face sandstones form in response to fair-weather reworking by near-shore current with coarsening upward sequence, which tends to be blocky at the top. It is rare to find any shale. Middle shore face sand is sandwiched between lower shoreface and upper shoreface sands. There is intercalation of shale in the body of sand and also coarsens upward. Lower shoreface sand is characterized by very dirty sand and is dominantly typified by the facies such as hummocky cross-stratification and fine-grained sands (Adeyemo et al., 2005). The beds show varying degrees of burrowing, and shale laminations are often completely fragmented by bioturbation. It has a considerable amount of marine deposit (shale) interbedded with sand

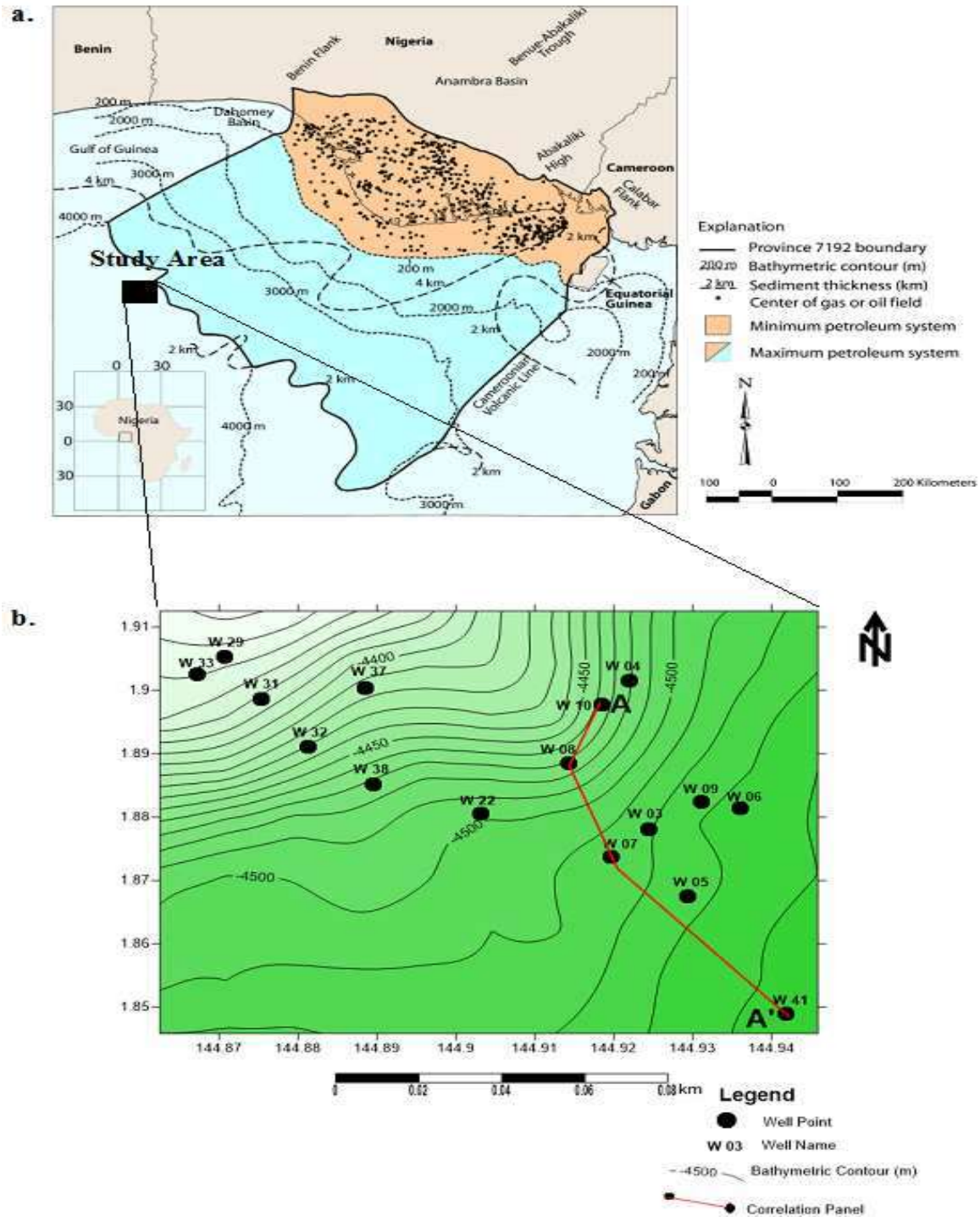

Fig. 1: (a) Map of the Niger Delta showing Province outline (Petroconsultants, 1996) (b) Location map of the study area which comprises a bathymetric map overlain by the location of all the wells, contours and a transverse for the correlation panel.

.

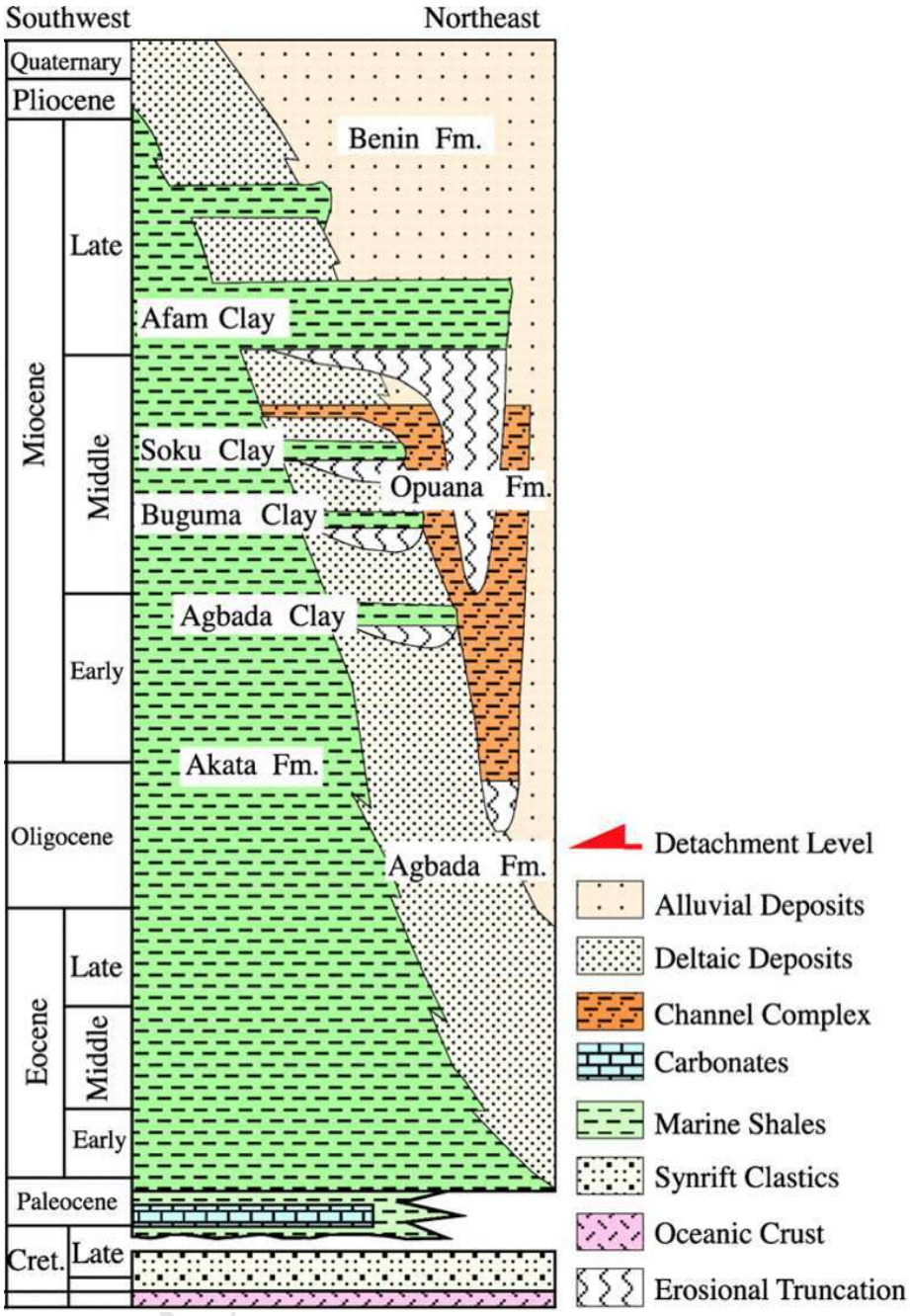

Fig. 2. Stratigraphic column showing formations of the Niger Delta (Modified from Doust and Omatsola, 1990).

3. Materials and methods

3.1 Data Gathering

The data used for this study are from the clastic reservoirs in the Niger Delta Basin (Fig. 1). Thirty five (35) well log data were available, 3 were bad, 22 wells have complete wireline log data (e.g., gamma, resistivity and neutron-density logs) while the remaining 10 wells limited log data (gamma, resistivity and neutron logs). After the well data were quality controlled, 21 of the wells were found suitable for this study. Consequently, the main hydrocarbon sands in the field are designated as D-03, G-01, G-04, G-07, H-01, H-04, J-10, J-17, and J-20 sands. The G-01 sand was used in the analysis because as it contains core data. A correlation panel of the G-01 sand across wells 10, 08, 07 and 41 is shown in Fig.1b while the cross section of the same wells is presented in Fig.3.

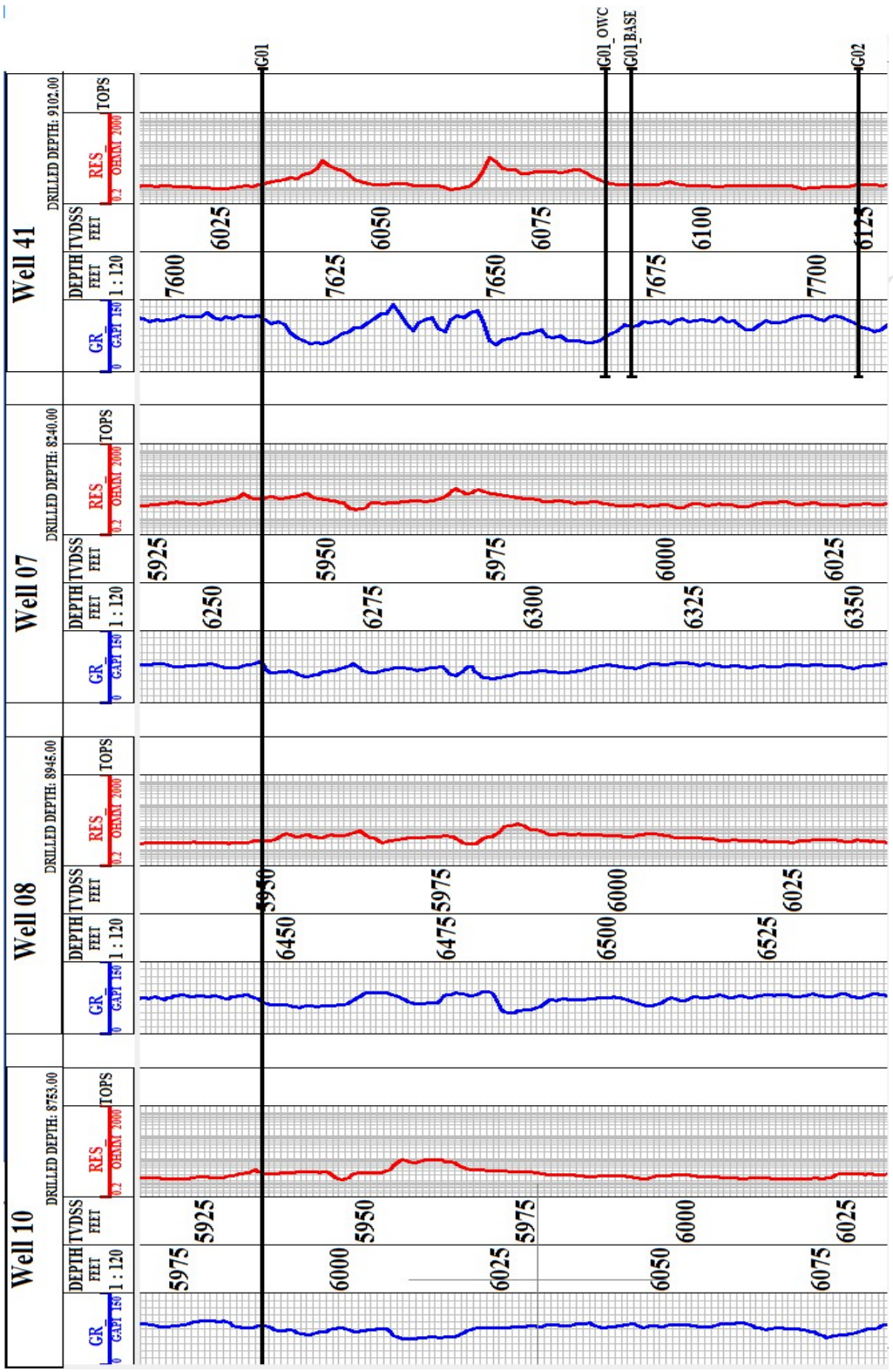

Fig. 3. Cross section of G-01 sand across wells 10, 08, 07 and 41.

3.2 Data validation / quality control

Core data were used for validation /quality control (Fig. 4a). Density log in cored well 41 was validated because it is a sensitive log in the calculation of total porosity and was used for modeling G-01 sand in other wells. Core porosity (POR_2) and apparent density from core (RHOB_A_2) as obtained in the expression in equation 1 shows good agreement with the actual density (RHOB) in cored well 41(Fig. 4b).

RHOB_A_2 = core. grain density – core. porosity * grain density + core. Porosity (1)

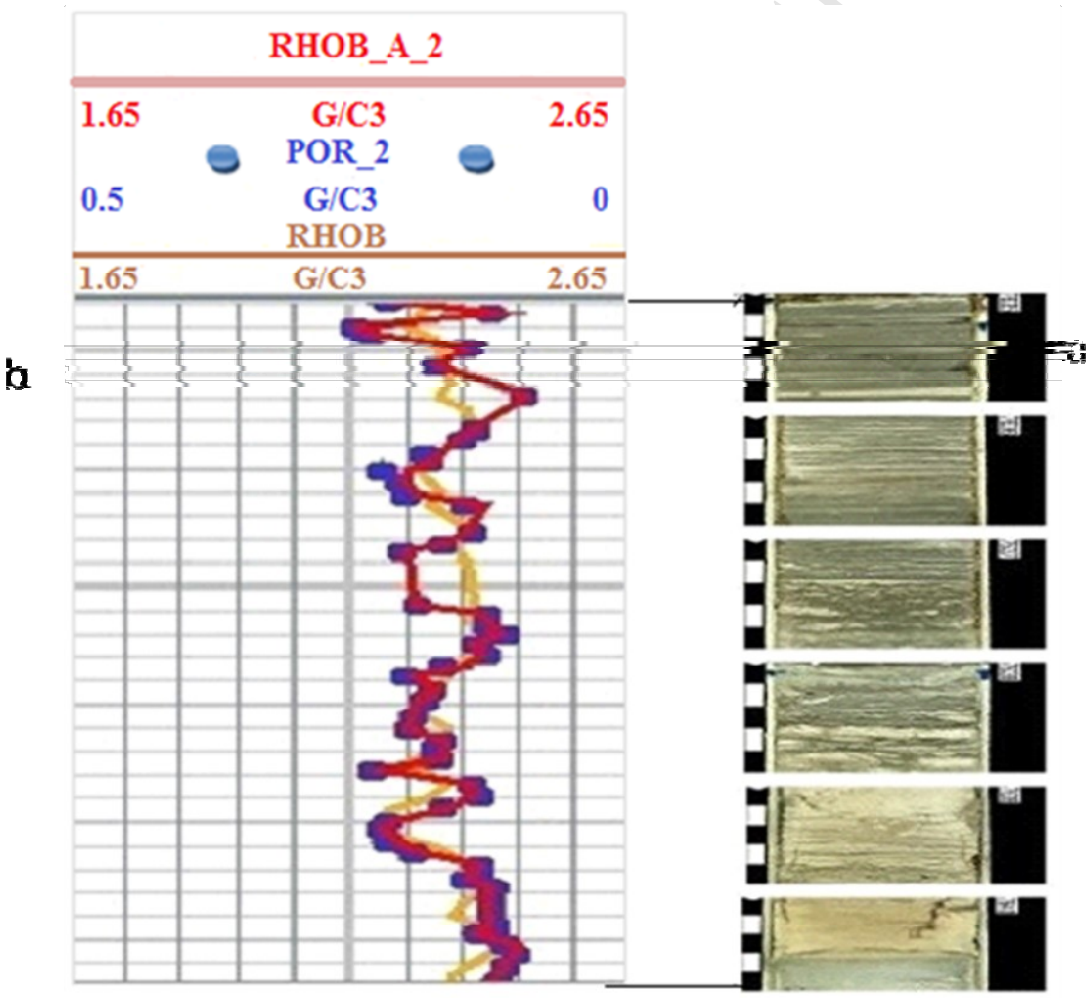

Fig. 4: a. core photographs of G-01 sand at depth interval 7650ft. – 8150ft. b. Log showing the agreement between the two validation techniques and the actual density (RHOB) in cored well 41.

3.2 Water saturation analysis from Archie equation

The water saturation (S_w) from Archie equation (Archie, 1942) as shown in equation 2 was used for conventional method

$$S_w = \left[\frac{a}{\phi^m} \frac{R_w}{R_t} \right]^{\frac{1}{n}} \quad (2)$$

where, a = tortuosity factor = 1.0, m = cementation exponent = 1.8, R_t = true resistivity, Ωm, R_w = formation water resistivity, Ωm, ϕ = porosity fraction, n = saturation exponent = 2.

The workflow in respect for the saturation height function and the estimation of hydrocarbon pore volume is presented as a flow chart in Fig.5. The details of the flow chart are presented in sections 3.3-3.7.

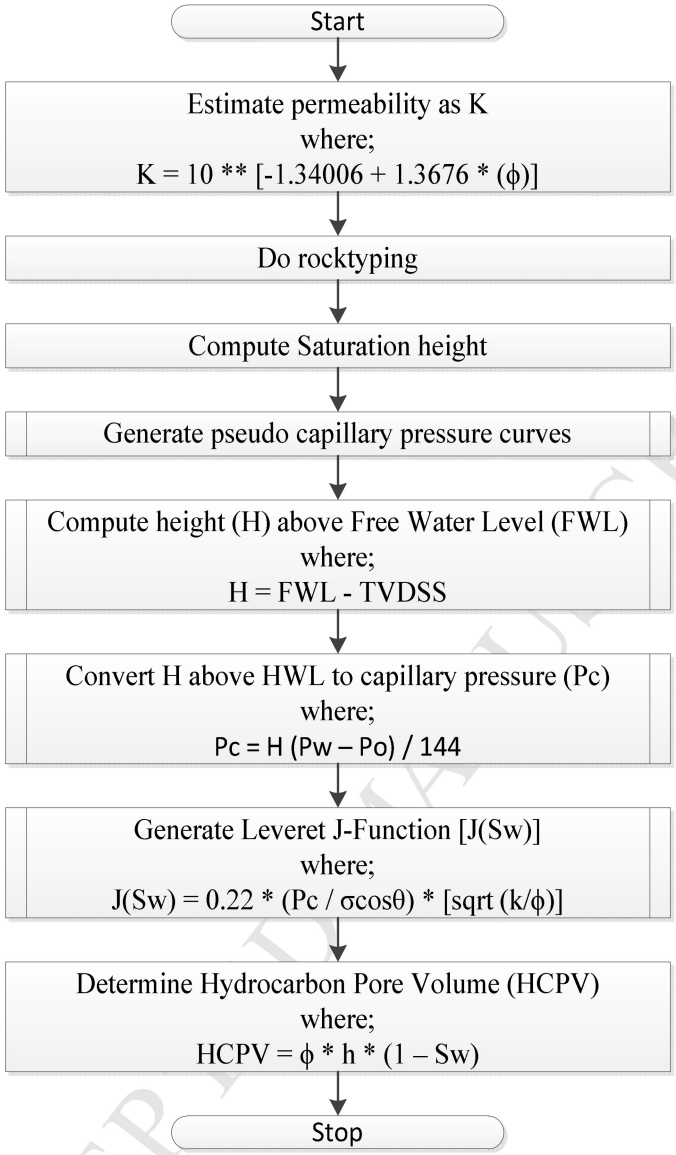

Fig.5. Flowchart showing the sequence for the estimation of permeability for computation of hydrocarbon pore volume.

3.3 Permeability

Permeability is not directly related to porosity; therefore, it cannot usually be determined from porosity alone (Adeoti et al., 2011). There is often a high correlation observed between porosity and permeability, particularly in sandstones and granular limestones (Adeoti et al., 2011). Then, an improved predictive relationship may be obtained when additional independent variables such as shale indicator are included. Hence, in this study, permeability was developed from the cored well 41. Fig. 6a shows the application of crossplot regression to the plot of core permeability (corex.kh) against core porosity (corex.por_2) before being filtered and this plot could not be used for permeability

development because it was affected by lamination. The regression equation from Fig.6b was obtained from the application of crossplot regression to the plot of horizontal core permeability (corex.kh) against core porosity (corex.por_2) filtered by core permeability (corex.kh)>4.

$$y = 10^{**} (- 1.34006 + 1.3676 *(x)) \quad (3)$$

Then volume of shale was used to define lithology. Then equation 3 was rewritten as

$$K = 10 ** (- 1.34006 + 1.3676 * (\phi)) \quad (4)$$

Total porosity (ϕ) derived from neutron/density data corrected to core porosity (phitc_nd_1) was substituted for x in the equation 3 to get y as permeability (k_nd_1). This was applied to all the wells having neutron and density logs.

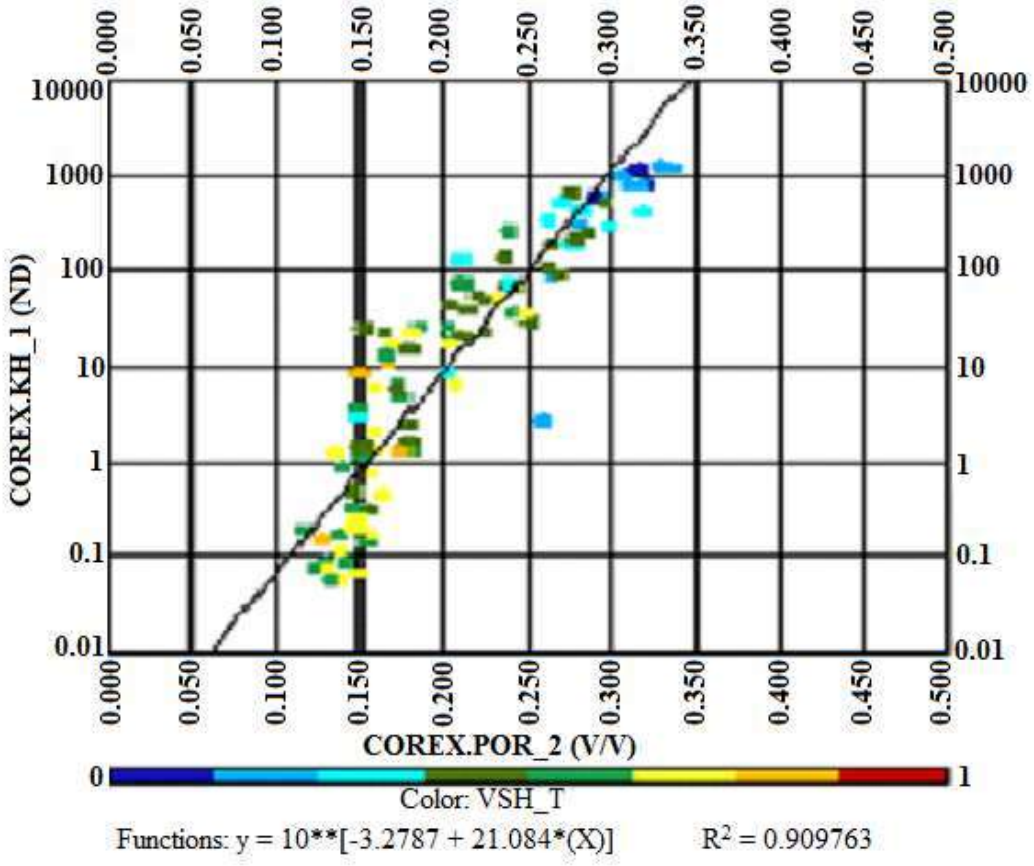

Fig. 6 (a). Plot of core permeability (COREX.KH_1) vs core porosity (COREX.POR_2) before being filtered.

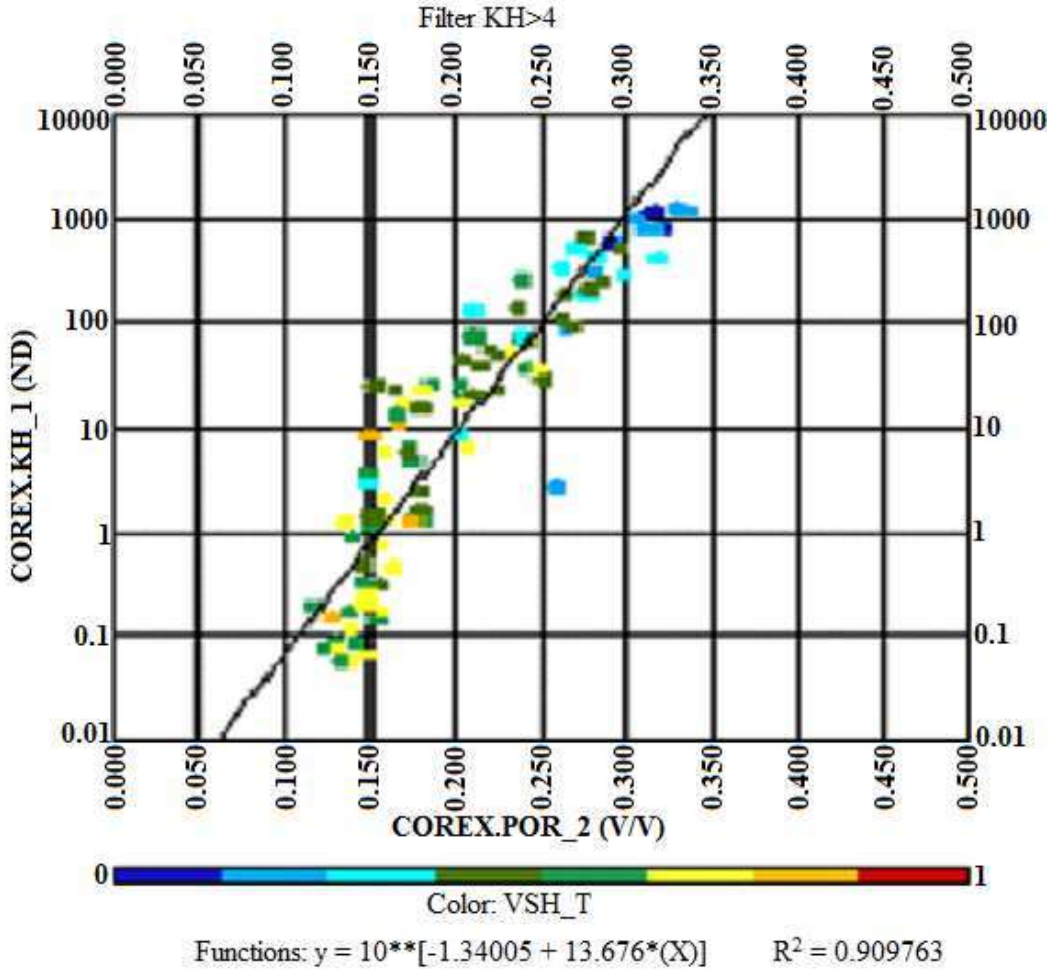

Fig. 6(b). Plot of core permeability (COREX.KH_1) vs core porosity (COREX.POR_2) after being filtered.

3.4 Rock type

Rock typing is a process of classifying reservoir rocks into distinct units, each of which was deposited under similar geological conditions and have undergone similar diagenetic alterations (Guo et al., 2005). The rock types derived in this study do not represent units deposited under similar geological conditions and have classified based on similar wireline log responses. Hence, they are pseudo rock types. The absolute value of permeability for a given porosity range can vary widely from one reservoir or rock type to another. Also within a reservoir, there can still be variation. The analysis for rock type development in this study was based on the plot of permeability (k_nd_1) against total porosity (phitc_nd_1) colored by volume of shale.

3.5 Saturation height functions

In this work, the saturation height functions are used to check that the log-derived water saturation is correct, generate water saturations in geological models away from well control and determine what the original water saturation was when the wells were drilled post production. The capillary pressure could be obtained from either special core data or logs (e.g., Leverrett,1941; Johnson, 1987; Cuddy et al., 1993; Skelt and Harrison,1995; Geir and Johne, 2000; Harrison and Jing, 2001; Adams, 2003; Juan et al., 2003; Anijekwu et al., 2004; Shawket et al., 2004; Amabeoku et al, 2005; Bech et al., 2005; Biniwale, 2005; Egermann et al., 2005; Guo et al., 2005; and Joanne et al., 2014). Due to the absence of special core data in the Orire Field and the need to have continuous water saturation throughout the formation thickness, water saturation was thus developed from pseudo capillary pressure curves generated from the use of modern wells with complete log data in the field.

3.5.1 Water saturation from pseudo capillary pressure curves

3.5.1.1 Pseudo capillary pressure curves

The pseudo capillary pressure curves were made based on the relationship between depth, Archie water saturation, sand on sand and rock type. The rock type was used to characterize the zonation of capillary pressure curves and was used to relate rock sample to the properties of the reservoir. Six wells (05, 06, 07, 22 29 and 41) were considered for the plot as they have the four rock type zones. Additionally, the plot was used to predict free water level (FWL) at 6085 ft.

3.5.1.2 Determination of height above FWL

Each curve was digitized at different depths above FWL with their water saturation values. The depth intervals were subtracted from FWL to obtain height above the FWL (H) as shown in equation 5.

$$H = FWL - TVDSS \tag{5}$$

3.5.1.3 Conversion of height above FWL to capillary pressure

The pressure gradients for the oil and water phases are determined by the fluid densities. The S_w distribution above FWL is controlled by the balance of pressure and buoyancy (gravity and density difference) forces. Then the capillary pressure (Pc) and height (H) are related by equation (6) of Harrison and Jing (2001),

$$p_c = \frac{H(\rho_w - \rho_o)}{144} \tag{6}$$

where ρ_w and ρ_o are the water and oil densities, respectively.

In this analysis, height above FWL was converted to the capillary pressure (P_c) by using equation (6), once height above FWL has been estimated (equation 5).

3.5.1.4 Capillary application of J-function in analyzing pseudo pressure data

The J- function has been applied for the analysis because it accounts for differences in rock types. The leveret J-function (Leverett, 1941) is written as

$$J(S_w) = 0.22\frac{Pc}{\sigma\cos\theta}\sqrt{\frac{k}{\phi}} \quad (7)$$

K is permeability (md), σ is interfacial tension between the fluids in dynes/cm, θ is the contact angle relating wettability and rock-fluid interaction in degrees and ϕ is porosity. The Leverett J-function has the effect of normalizing all curves to approach a simple curve and is based on the assumption that the porous medium can be modelled as a bundle of non-connecting capillaries (Leverett, 1941). Obviously, the more the capillary bundle assumption deviates from reality, the less effective the J-function correlation becomes. The correlation is not unique but seems to work better when the rocks are classified as rock types. The Leverett J-function has been widely used as a correlating group for all capillary pressure measurements using different fluid systems but it only applies if the porous rock types have similar pore size distributions or pore geometry. For a set of samples with similar pore size distribution, a least square regression analysis is then made using the J-values as the independent variable. The best correlation is often obtained using a power law equation of the form (Harrison and Jing, 2001)

$$J = a\ (Sw)^b \quad (8)$$

The derived J-function now becomes a master curve that can be used to represent the reservoir and in the absence of other data can be used for other reservoirs of similar rock type. K and ϕ in equation 7 were obtained from the distribution of porosity and permeability in the reservoir from the histogram of porosity from neutron-density and the histogram of permeability derived from log filtered by four rock types. The mean of the frequency curves was considered for choosing porosity and permeability in each zone. Then, the results are shown in Table 1. The values of $(\rho_w, \rho_0, \sigma, \theta)$(Core laboratories, 1941) used in this study are presented in the Table 2.

Table 1. Results of the mean of the frequency curves considered for porosity and permeability in each rock type zone.

Rock type (rtyp)	Porosity (por) (frac.)	Permeability (K) (md)
1	0.35	3508
2	0.304	768
3	0.248	107
4	0.18	10.5

Table 2. Contact angle, interfacial tension and density variation for fluid pairs. Contact angle and interfacial tension for average reservoir (Core laboratories, 1982).

Parameters	Units	Values
Reservoir interfacial tension (σ)	dyne/cm	30
Reservoir contact angle (θ)	degree	30
Reservoir σcosθ	dyne/cm	26
Density of water (ℓw)	Ib/cuft	62.4
Density of oil (ℓo)	Ib/cuft	46.8

By using porosity and permeability derived from logs and pseudo pressure data, J values for the four rock types were estimated. Thereafter, the non-linear regression (power law) was applied to the plots of water saturation values from 4 rock types against corresponding J function values to obtain water saturation for the four rock type zones.

3.6 Determination of hydrocarbon pore volume

Hydrocarbon pore volume (HCPV) from Archie and J-function results was determined to predict sand qualities from equation 9 (Bateman, 1990),

$$HCPV = \phi * h * (1 - S_w) \quad (9)$$

where h = net pay (ft)

4. Results and discussion

4.1 Results

4.1.1 Characterization and analysis of rock types

The plot of permeability against total porosity from neutron-density led to the characterization of permeability into five zones by the volume of shale (Fig. 7). The different rock types with their permeabilities are presented in Table 3. Rtyp 5 was not considered for further analysis because it is totally shale. The different rock type zones delineated are rock type 1 to 5 (Fig. 8). While owing to five classes of grain sizes with each occupying a fairly range of permeability, rocktype 1 can be likened to lower medium sand while rock type 2, rock type 3, rock type 4 and rock type 5 are diagnostic of lower – upper fine sand, lower very fine sand, burrowed very fine shaly sand and shale respectively..

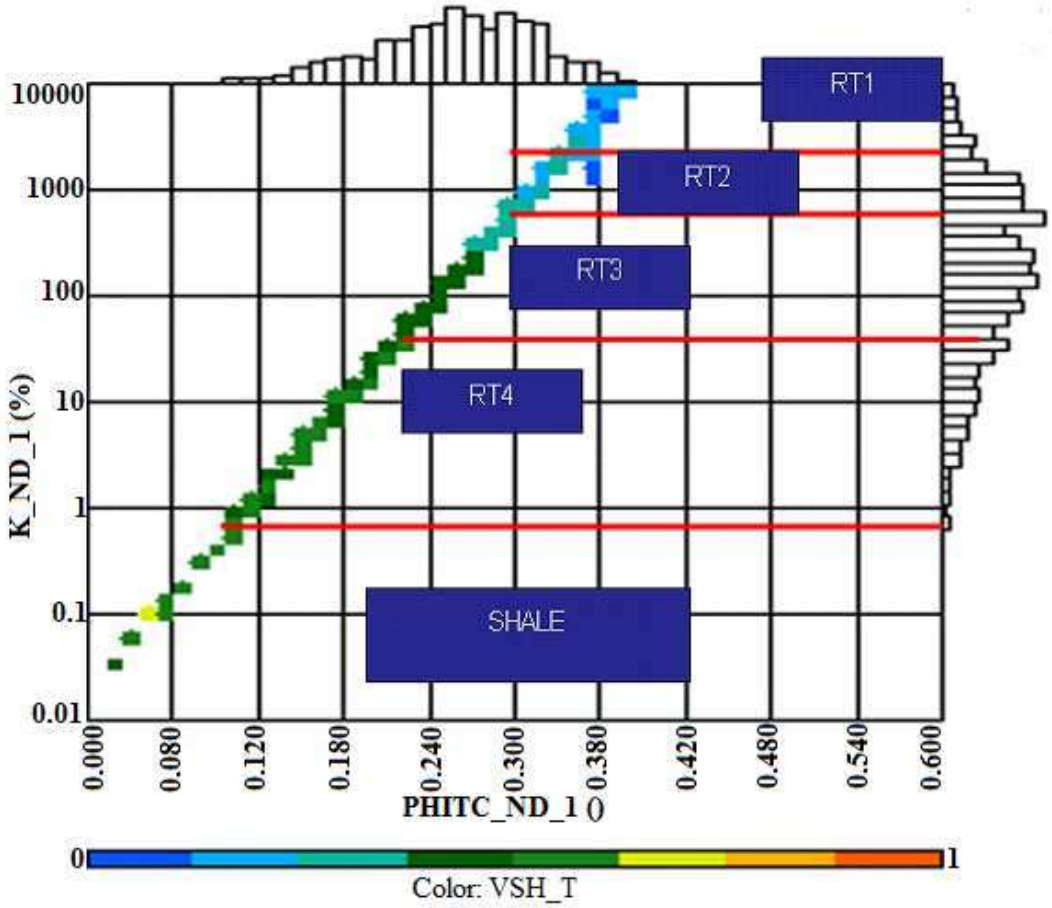

374

375 Fig.7. Plot of permeability (K_ND) vs total porosity (PHITC_ND) for rock type
376 characterization.

377

378 Table 3. The different rock types with their permeabilities and colours

Rocktype (Rtyp)	Permeability (K_nd_1) md	Colour
Rtyp 1	> 1533	Yellow 3
Rtyp 2	> 324 and < 1533	Wheat
Rtyp 3	> 31 and < 324	Burlywood
Rtyp 4	> 2 and < 31	Sienna
Rtyp 5	< 2	gray4

379

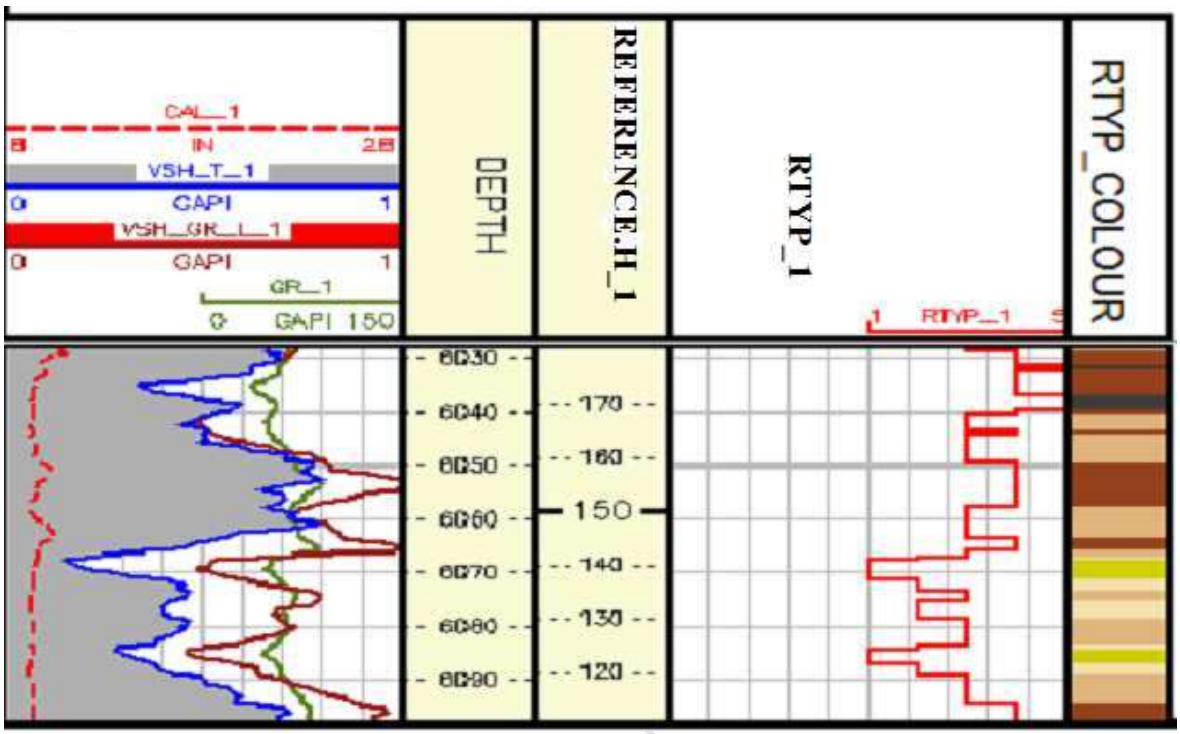

Fig.8. A log sample indicating the five rock types: - Yellow 3, Rtyp 1; - Wheat, Rtyp 2; - Burlywood, Rtyp 3; -Sienna, Rtyp 4; - Grey4, Rtyp 5.

4.1.2 Generation of water saturation profiles from pseudo capillary pressure data

The four rock types exhibit distinct J-function profiles (Fig. 9 a-d) and their corresponding Sw equations are:

i. $S_w = 0.5934\ J^{-0.327}$ for rock type 1,

ii. $S_w = 0.6942\ J^{-0.223}$ for rock type 2,

iii. $S_w = 0.7416\ J^{-0.135}$ for rock type 3

iv. $S_w = 0.8554\ J^{-0.057}$ for rock type 4.

The composite S_w profile (S_w2) was generated based on the distribution of the four rock types within the reservoir using four S_w equations obtained from Fig.9 a-d.

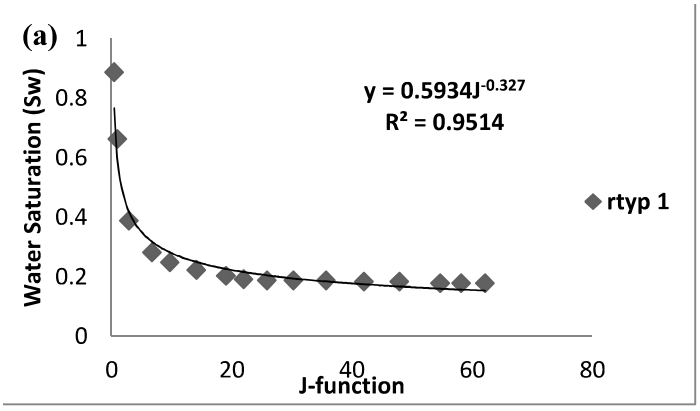

397
398
399

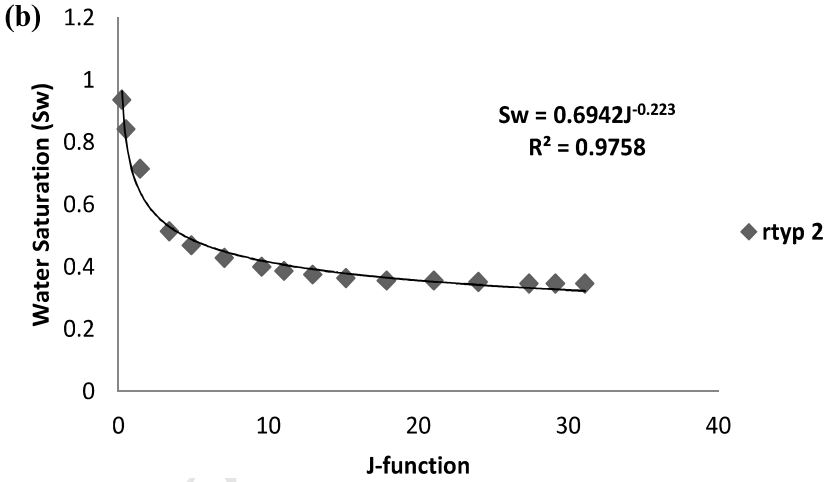

400
401
402
403
404
405
406

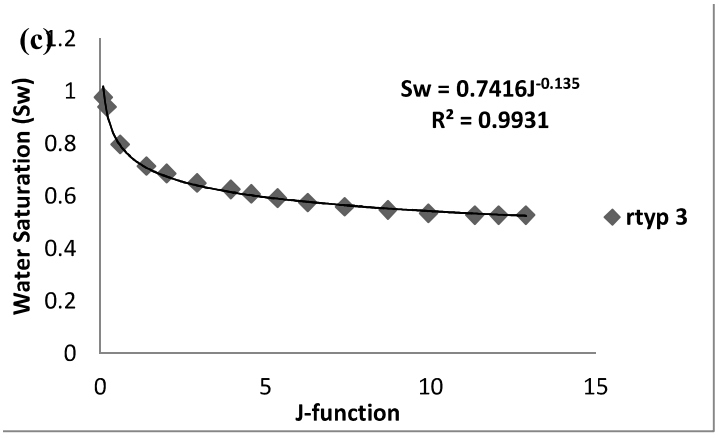

407

408

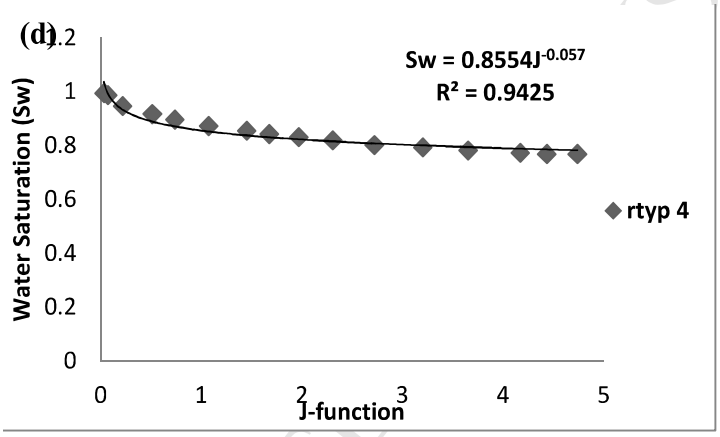

409

410

411 Fig. 9: J-function curves (a) rock type 1 (b) rock type 2 (c) rock type 3 (d) rock type 4.

412 .

413 **Then, J – function formula (equation 7) was substituted into four S_w equations from**

414 **the four rock types (**Figs. 6a to 6d) as shown in equations 10-13.

415 $$\text{rtyp} = 1, S_w = 0.5934\left[0.22\frac{Pc}{\sigma\cos\theta}\left(\frac{k\_nd}{phitc\_nd}\right)\right]^{-0.3274} \quad (10)$$

416 $$\text{rtyp} = 2, S_w = 0.6942\left[0.22\frac{Pc}{\sigma\cos\theta}\left(\frac{k\_nd}{phitc\_nd}\right)\right]^{-0.2228} \quad (11)$$

417 rtyp = 3, $S_w = 0.7416\left[0.22\frac{Pc}{\sigma\cos\theta}\left(\frac{k\_nd}{phitc\_nd}\right)\right]^{-0.1353}$ (12)

418 rtyp= 4, $S_w = 0.8554\left[0.22\frac{Pc}{\sigma\cos\theta}\left(\frac{k\_nd}{phitc\_nd}\right)\right]^{-0.0574}$ (13)

419

420 Thereafter, Equations 10 through 13 were collapsed into one to obtain S_w2 (water
421 saturation from pseudo capillary pressure curves) from the four rock type zones within a
422 rock type by interpretation software (Geolog). S_w2 is the water saturation from the
423 combination of the four rock type zones. The S_w2 generated from the four rock type
424 zones was now applied to the logs to verify the resistivity based water saturation
425 (sw_arch_nd)

426

427 **4.2 Discussion**

428 *Comparison of the water saturation from the two models*

429 Figure 10a (well 05) shows good agreement between the water saturation from the
430 resistivity based method and the one from pseudo capillary pressure because the wells are
431 modern and have good set of log data, especially in oil zone. Figure 10b (well 13)
432 depicts where the resistivity equipment failed, which led to the cutting off of a part of the
433 resistivity log, then S_w2 result can be used for its replacement i.e. the uncertainty
434 identified has been taken care by S_w2. Fig. 10c (well 31) describes where the S_w value
435 from the resistivity based method is higher than that of S_w2, it was discovered that old
436 resistivity tools with poor resolution were run. These old logs are just inaccurate and
437 cannot measure the correct formation resistivity thereby underestimating the hydrocarbon
438 saturation. S_w2 was now used to verify the result, i.e. reduce the uncertainties associated
439 with S_w from historical resistivity based method. S_w2, therefore, captures the hydrocarbon
440 ignored by resistivity based method because it accounts for difference in rock types. Fig.
441 10d (well 41) shows that S_w2 is higher than S_w from resistivity based method in some
442 parts of the reservoir because the height above the FWL is very close to the OWC. S_w2
443 validates the fact that if height above FWL is very close to the OWC, higher pressure will
444 be needed to draw water from the reservoir (Okolie and Ujanbi, 2007); therefore, water
445 saturation from pseudo capillary pressure will be higher than water saturation from

resistivity based method. Fig. 10e (well 03) reflects that where the S_w values from the resistivity based method is lower than that of S_w2, the uncertainties were attributable to old resistivity tools cum effects of cementation factor 'm' which could be further investigated by using special core data.

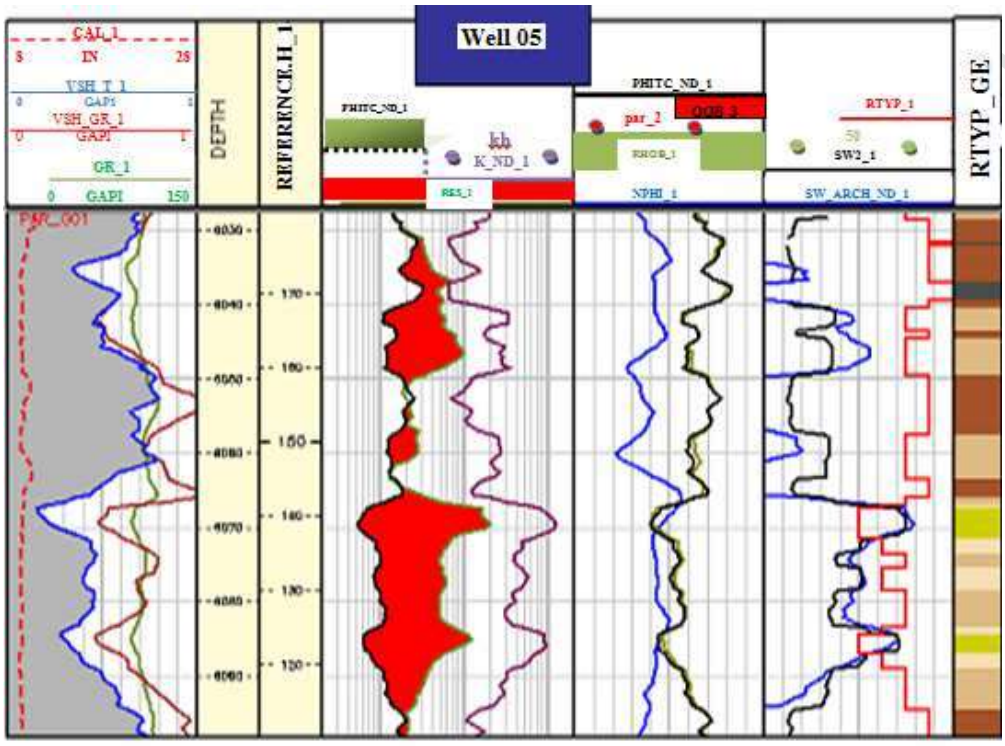

Fig. 10a. Composite log showing an agreement between Archie water saturation and S_w from Pc curves.

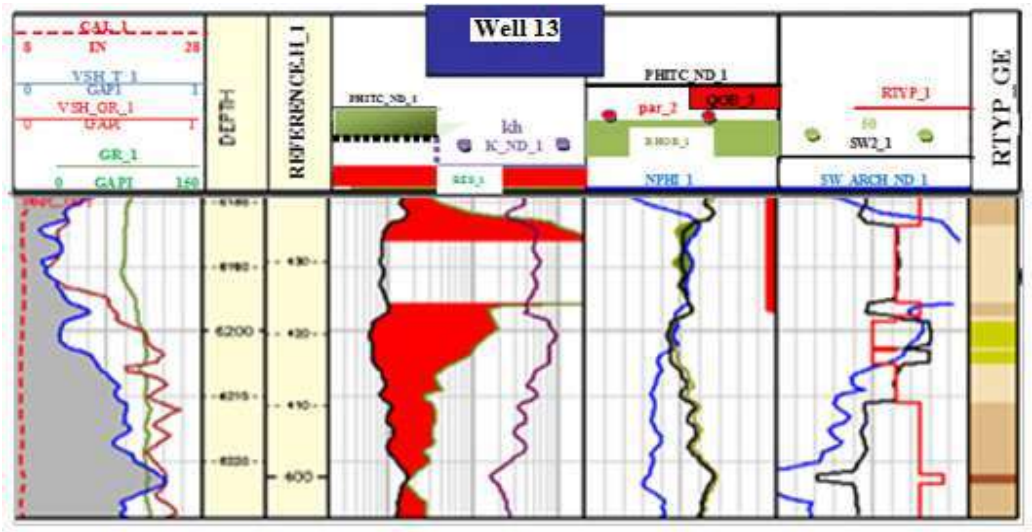

Fig. 10b. Composite log showing failed resistivity tool which made S_w from Archie unknown.

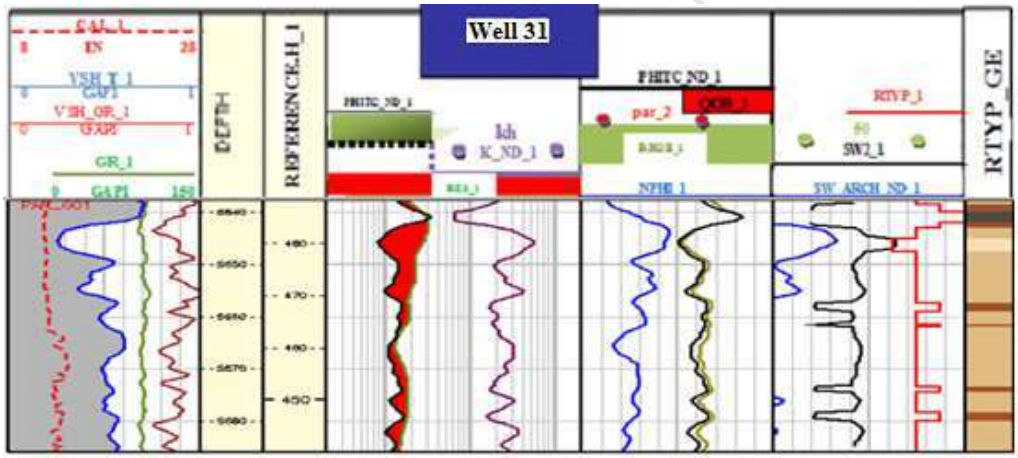

Fig. 10c. Composite log showing poor resolution of resistivity tool which overestimates Archie water

saturation

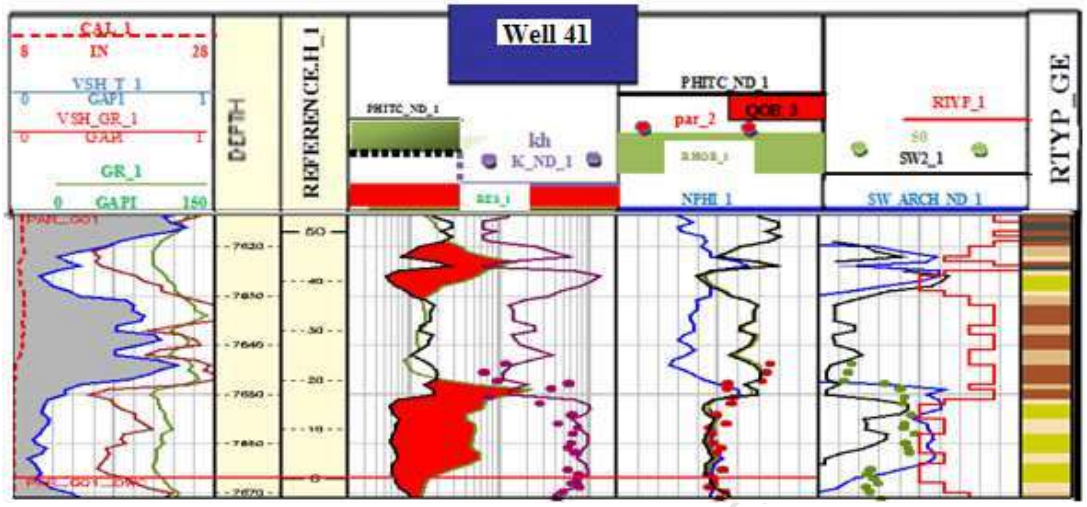

Fig. 10d.Composite log showing that the height above FWL is closer to OWC, then S_w from Pc curves is higher than S_w from Archie.

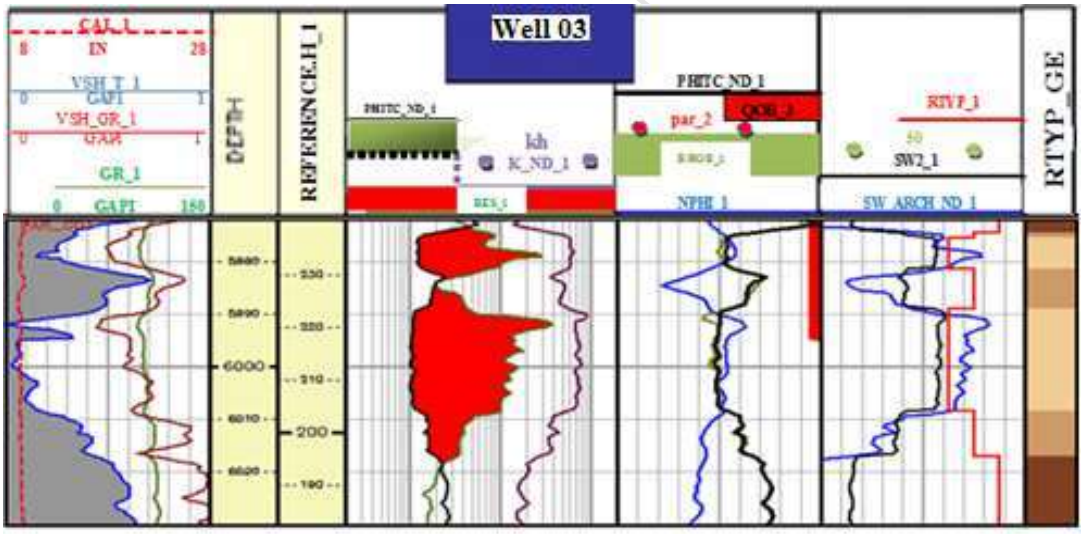

Fig. 10e. Composite log showing the uncertainties attributable to old resistivity tools cum effects of cementation factor 'm' where S_w from resistivity log is lower than SW2.

Analysis of hydrocarbon pore volume

Table 4 shows the results of hydrocarbon pore volume from Archie (HCPV_A) and J-function (HCPV_J). The plot of hydrocarbon pore volume values from both methods (Fig. 11) reveals that wells with high HCPV have high sand qualities while those with low HCPV have low sand qualities. Also, the geometry of the stratigraphic units could be deduced from the plot.

Table 4. Hydrocarbon pore volume from Archie (HPV_A) and J-function (HPV_J) values.

WELLS	01	02	03	04	05	06	07	08	09	10	13	22	29	31	32	33	
HCPV_A	7.59	12.73	6.12	10.68	4.75	9.52	2.36	3.66	6.72	7.34	3.94	6.01	6.78	2.83	1.57	0.20	0
HCPV_J	9.09	15.00	5.86	9.82	4.74	9.24	2.18	2.61	5.68	5.51	6.40	6.09	8.76	7.07	4.68	3.64	4

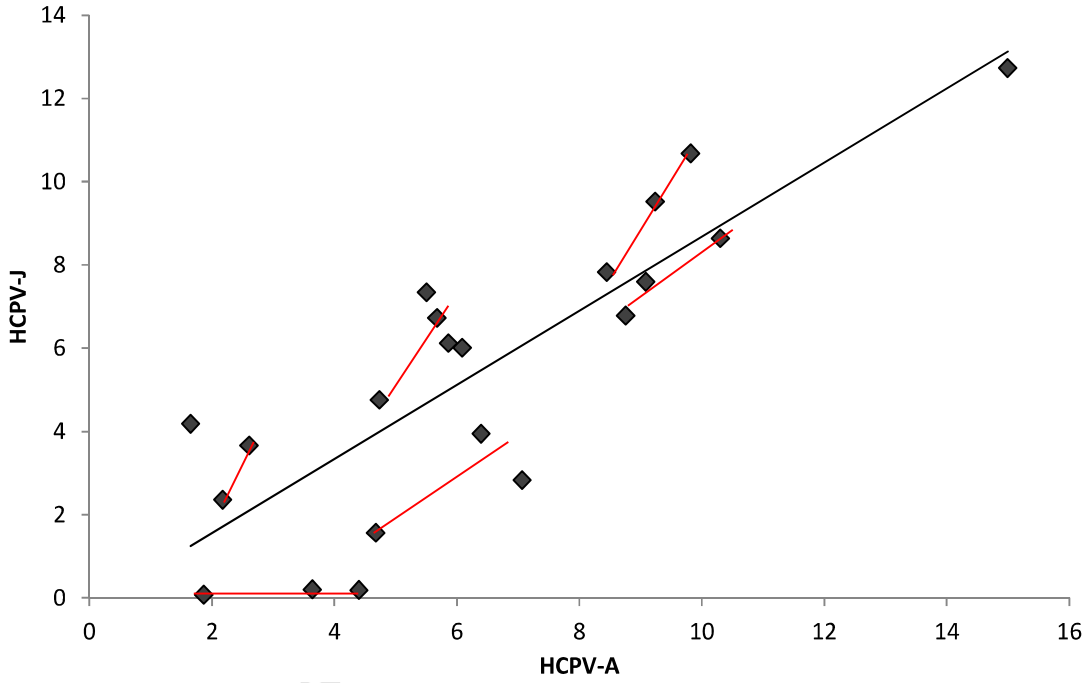

Fig. 11. Plot of hydrocarbon pore volume from J-function (HCPV_J) vs hydrocarbon pore volume from Archie (HCPV_A).

Implication for hydrocarbon exploration in the Niger Delta and other similar basins

The saturation height function has assisted to address the issues of overestimating the water saturation values in G-01 sands which eventually led to the discovery of more hydrocarbons. This method could be applied to other reservoirs within the Niger Delta province where similar problem is experienced. The model here could be used to generate water saturations in geological models away from well control, or determine what the original water saturation was when wells have been drilled post production. In addition, this model could also be applied to reservoirs of similar rock type in other fields which belong to the clastic environment. Apart from the Niger Delta, Guo et al., 2005 have

applied saturation height function in clastic reservoir in the Oriente Basin ,South America to show that consistent initial water saturation models (i.e., calculated and log measured water saturations are in excellent agreement) could be obtained when the proper J-function is used for a given rock type. These authors further stressed that uncertainty associated with volumetric calculations could be greatly reduced as a more accurate initial water saturation model was used.

5. Conclusions

This study has equally shown that the alternative method of generating water saturation from pseudo capillary pressure curves called saturation height function is a potential algorithm for calculating water saturation (S_w) as a function of height above the free water level. This model was further used to relate each capillary pressure curve to each rock type zone. Comparison of water saturation from resistivity model with water saturation from pseudo capillary pressure curves shows that where the wells have good set of log data, the results of water saturation from both methods show good agreement. However, in wells where the results of water saturation from historical resistivity method are doubtful due to uncertainties arising from bad resistivity log and poor resolution of old resistivity tools, saturation height function provides accurate water saturation. In addition, the plot from the computation of hydrocarbon pore volume (HCPV) from Archie and J-function shows that wells with high HCPV have high qualities while wells with low HCPV have low sand qualities. The algorithm presented here can be applied to reservoirs of similar rock type in other fields or frontier basins.

Acknowledgement

The authors want to thank Department of Petroleum Resources and Chevron Nig Ltd for their permission to publish this article. In addition, we would like to acknowledge the support of Mr Tad Schirmer, Mr Felix Udegunam, Dr John Crowne and Mr Zalan Thomas for their invaluable contributions

References

Adams, S., 2003. Modelling imbibition capillary pressure curves. In: the Annual Technical Conference and Exhibition, SPE paper 84298. October 5–8, Denver, Colorado, USA.

Adeoti, L., Adole, S.A., Zalan, T., Onyeji, J.A., 2011. Rock-typing d evelopment (RTD) – A tool for enhanced reservoir characterization (A case study of "ADSA FIELD" in the Niger Delta, Nigeria). Nigerian Association of Petroleum Explorationists (NAPE) Bulletin, 23(1), 31-37.

Adeyemo, Dapo., Logan, James. P., Saha, Souvick., 2005. Enhanced clay characterization and formation evaluation with wireline spectroscopy tool: Examples from Nigeria. In: 46th Annual Logging Symposium, SPWLA paper, June 26 – 29, New Orleans, Louisiana,USA

Amabeoku, M.O., Kersey, D.G., Bin-Nasser, R.H., Al-Waheed, H.H., Belowi, A.R., 2005. Incorporating hydraulic units concepts in saturation-height modeling in a gas field. In: Proceedings of SPE Asia Pacific Oil & Gas Conference and Exhibition, April 5-7, Jakarta, Indonesia.

Anijekwu, C., Odegbesan, C.O., Ogagarue, E.E.E., 2004. Regional correlation on saturation height function for Niger Delta oil province. In: Proceedings of SPE Annual International Technical Conference and Exhibition, August 2–4, Abuja, Nigeria.

Archie, G.E., 1942. The electrical resistivity log as an aid in determining some reservoir characteristics. Trans. Am. Inst. Min. and Metall. Eng. 146, 54 - 62.

Avbovbo, A.A., 1978. Tertiary lithostratigraphy of the Niger Delta. American Association of Petroleum Geologists Bulletin. 62, 295 - 307

Bateman, R., 1990. Open Hole Log Analysis and Formation Evaluation. Texaco Exploration and Production Technology Division, Houston Texas.

Bech, N., Frykman, P., Vejbaek, O.V., 2005. Modeling of initial saturation distributions in oil/water reservoirs in imbibition equilibrium. In: Proceedings of Society of Petroleum Engineers, Annual Technical Conference and Exhibition, October 9–12, Dallas, Texas, USA.

Biniwale, S., Behrenbruch, P., 2005. An improved approach for modelling geological

562 depositional characteristics and fluid saturation by using hydraulic units,
563 Australian offshore fields. In: 46th Annual Technical Meeting of the Society of
564 Petrophysicists and Well Log Analysts; June 26–29, New Orleans, USA.
565 Core Laboratories 1982. A course in special core analysis study. Dallas, Texas.
566 Cuddy, S., Steele, R., Allinson, G., 1993. The foil function – a sample, convincing model
567 for calculating water saturations in southern north sea gas fields. In: 34th Annual
568 Logging Symposium of the Society of Professional Well Log Analysts. June 1-17,
569 Calgary, Canada.
570 Dewan, J.T., 1983. Essentials of modern open-hole log interpretation, PennWell
571 publishing company, Oklahoma.
572
573 Doust, D.M., Omatsola, E., 1990. Niger Delta. *In: Divergent/Passive Margin Basins*. J.D.
574 Edwards., P.A. Santogrossi, editors. AAPG Memoir 48. American Association of
575 Petroleum Geologists, Tulsa, USA, 239 – 248
576 Egermann, P., Lombard, J.M., Fichen, C., Rosenborg, E., Tachet, E., Lenormand, R. A.,
577 2005. New experimental method to determine interval of confidence for capillary
578 pressure and relative-permeability curves. In: Proceedings of Annual Technical
579 Conference and Exhibition of the Society of Petroleum Engineers. October 9-10,
580 Dallas, Texas, USA.
581 Ejedawe, J.E., Coker, S.J.L., Lambert-Aikhionbare, D.O., Alofe, K.B., Adoh, F.O., 1979.
582 Evolution of oil-generative window and oil and occurrence tertiary Niger-Delta
583 basin. American Association of Petroleum Geologists. 68, 1574 – 1585
584 Ekweozor, C.M., Daukoru, E.M., 1984. Petroleum source bed evaluation of Tertiary
585 Niger Delta. American Association of Petroleum Geologists Bulletin. 68, 390 –
586 394
587 Ekweozor, C.M., Okoye, N.V., 1980. Petroleum source-bed evaluation of tertiary Niger
588 Delta. American Association of Petroleum Geologists Bulletin 64, 1251 - 1259
589 Evamy, B.D., Haremboure, J., Kamerling, P., Knaap, W.A., Molloy, F.A., Rowlands,
590 P.H., 1978. Hydrocarbon habitat of tertiary Niger Delta. American Association of
591 Petroleum Geologists (AAPG) Bulletin, 62, 1 - 39.
592 Geir, T.E., Johne, A.L., 2000. Numerical modeling of capillary transition zones. In:
593 Proceedings of Asia Pacific Oil and Gas Conference and Exhibition of the Society
594 of Petroleum Engineers, October 1-13, Brisbane, Australia.

595 Goetz, J. F., 2002. Well Log Interpretation. PetroSkill LLC, Tulsa, Oklahoma.
596 Guo, G., Diaz, M.A., Paz, F., Smalley, J., Waninger, E.A., 2005. Rock typing as an
597 effective tool for permeability and water-saturation modeling, a case study in a
598 clastic reservoir in the oriente basin. In: Annual Technical Conference and
599 Exhibition of the Society of Petroleum Engineers paper SPE 97033, October 9-12,
600 Dallas, Texas, USA.
601 Haack, R.C., Sundararaman, P., Diejomahor, J.O., Xiao, H., Gant, N.J., May, E.D.,
602 Kelsch, K., 2000. Niger Delta petroleum systems, Nigeria. *In: Petroleum Systems*
603 *of South Atlantic Margins*. Mello, M.R., Katz, B.J., AAPG Memoir 73, 213 - 231.
604
605 Harrison, B., Jing, X.D., 2001. Saturation height methods and their impact on volumetric
606 hydrocarbon in place estimates. SPE paper 71326. In: Annual Technical
607 Conference and Exhibition of the Society of Petroleum Engineers. September 30-
608 October 3, New Orleans, Louisiana, USA.
609 Juan, C.G., Omar, A., Gabriel, P., Jean, F.M., 2003. Deriving capillary pressure and
610 water saturation from Nmr transversal relaxation times. SPE paper 81057. In:
611 Latin American and Caribbean Petroleum Engineering Conference of the Society
612 of Petroleum Engineers. April 27-30, Port-of –Spain, Trinidad, West Indies.
613 Joanne, T., Mike, L., Sarah, D., Millar, M.A., 2014. Novel integrated approach to
614 estimating hydrocarbon saturation in the presence of pore-lining chlorites. Pet.
615 Geosci. 20(2), 201-9.
616 Johnson, A., 1987. Permeability averaged capillary pressure. A supplement to log
617 analysis. In: Proceedings of 28th Annual Logging Symposium of the Society of
618 Professional Well Log Analysts, June 29th – July 2nd, London, England.
619 Kaplan, A., Lusser, C.U., Norton, I.O., 1994. Tectonic map of the world, Panel 10. Am.
620 Assoc. Pet. Geol. Tulsa.
621 Kogbe, C. A., 1989. The Cretaceous Paleocene Sediments of Southern Nigeria. In Kogbe,
622 C. A., (Ed.), Jos, Rock View Ltd. Geology of Nigeria 320–325.
623 Kulke, H. 1995. Nigeria. *In regional petroleum geology of the world. Part II: Africa,*
624 *America, Australia and Antarctica.* H. Kulke, editor. Gebrüder Borntraeger,
625 Berlin, Germany, 143 - 172
626 Lambert – Aikhionbare, D.O., Ibe, A.C., 1984. Petroleum source bed evaluation of
627 tertiary delta. AAPG Bulletin, 68, 387 - 394.

628 Leverett, M.C., 1941. Capillary behavoir in porous solids. Trans. Am. Inst. Min. Metall.
629 Eng. 142, 152-169.
630 Okolie, E.C., Ujanbi, O., 2007. Estimation of height of oil-water-contact above free water
631 level using capillary pressure method for effective classification of reservoirs in
632 the Niger Delta. Nigerian Journal of Physics, 19(2), 303 – 306.
633 Poupon, A., Leveaux, J., 1971. Evaluation of water saturation in shaly formations. The
634 Log Analyst, 7, 3-8
635 Peter, A.S., Darwin, S., 1982. Sandstone depositional environments. Am. Assoc. Pet.
636 Geol. 225 – 29.
637 Petroconsultants, 1996, Petroleum exploration and production database: Houston, Texas,
638 Petroconsultants, Inc., [database available from Petroconsultants, Inc., P.O. Box
639 740619, Houston, TX 77274-0619].
640 Robert., S.E., 2001. Encyclopedic dictionary of Applied Geophysics. 4th Edition. Soc.
641 Explor. Geophys. Tulsa, Oklahoma.
642 Schlumberger 1989. Log interpretation principle/applications. Schlumberger Well
643 Services, Houston.
644 Shawket, G.G., Bertrand, M.T., Douglas, A.B., 2004. Modelling and validation of initial
645 water saturation in the transition zone of carbonate oil reservoirs. In: Proceedings
646 of Abu Dhabi International Petroleum Exhibition and Conference of the Society
647 of Petroleum Engineers. October 10-13, Abu Dhabi, UAE
648 Short, K.C., Stauble, A.I. 1967. Outline of geology of Niger Delta. American Association
649 of Petroleum Geologists Bulletin. 51, 761 - 779
650 Simandoux, P., 1963. Dielectric measurements in porous media and application to shaly
651 formations. Revue de L'Institut Francais du Petrole, 18, (Suppl.Issue), 193-215.
652 Skelt, C., Harrison, B., 1995. An integrated approach to saturation height analysis. In:
653 Proceedings of Annual Logging Symposium of the Society of Professional Well
654 Log Analysts. June 26-29, Paris, France.
655 Stacher, P., 1995. Present understanding of the Niger Delta hydrocarbon habitat. *In:*
656 *Geology of Deltas.* Oti, M.N., Postma(eds)., A.A. Balkema: Rotterdam, The
657 Netherlands. 257 - 267.
658 Weber, K.J., Daukoru, E.D., 1975. Petroleum geology of the Niger Delta. Tokyo, 9th
659 World Petroleum Congress Proceedings, 2, 209 - 221.
660 Worthington, P.F., 2000. Recognition and evaluation of low-resistivity pay, Petroleum

661 Geosciences, 6, 77-92.

662

663

664

HIGHLIGHTS

- Saturation height function (Sw2) provides accurate water saturation.
- The plot of permeability against total porosity reveals five rock types.
- Sw2 can predict similar rock types in other fields within clastic environment. .
- The relationship between hydrocarbon pore volume and sand qualities is established.